Electron-impact excitation of the lowest four excited states of argon

N. T. Padial,* G. D. Meneses, F. J. da Paixão, and Gy. Csanak†
Instituto de Fisica "Gleb Wataghin," Universidade Estadual de Campinas, 13.100-Campinas-S. P., Brasil

David C. Cartwright
Theoretical Division, Los Alamos Scientific Laboratory, Los Alamos, New Mexico 87545

(Received 13 May 1980)

First-order many-body theory has been used to calculate the differential and integral cross sections for electron-impact excitation of the argon atom to the $4\,^3P_0$, $4\,^3P_2$, $4\,^3P_1$, and $4\,^1P_1$ electronic states, for incident electron energies of 16, 20, 30, 50, and 80.4 eV. The resulting cross sections are in good agreement with recent results extracted from electron energy-loss measurements on argon. Detailed calculations show that spin-orbit coupling must be included in the $^3P_1$ wave function in order to describe the electron-impact excitation of the state properly.

I. INTRODUCTION

The electron-impact excitation of the argon atom, first studied experimentally and theoretically in the 1930's, has been the subject of renewed scientific interest because of its important role in (for example) certain rare-gas discharge lasers.[1] The early experiments of Nicoll and Mohr[2] showed a characteristic diffraction pattern in the differential cross section (DCS) for excitation of the unresolved $4s[3/2]_1^0(^3P_1)$, $4s[3/2]_2^0(^3P_2)$, $4s'[1/2]_0^0(^3P_0)$, $4s'[1/2]_1^0(^1P_1)$ levels[3] for a wide range of energies. Massey and Mohr[4] were subsequently able to explain this pattern qualitatively, on the basis of a simplified form of the distorted-wave approximation (DWA), as due to the interference among various distorted waves. Their simplification of the DWA consisted of replacing the distorted waves by their asymptotic forms and calculating the scattering phase shifts in Jeffrey's approximation (also called the JWKB approximation).[5] The recent measurements of the DCS by Lewis *et al.*[6] (of the still unresolved $4s$, $4s'$ levels) confirmed qualitatively the earlier results of Nicoll and Mohr. For example, at 40 eV incident energy, the results of the two measurements are practically identical although the diffraction pattern became more pronounced (deeper minima) in the more recent measurements. Sawada *et al.*[7] have recently reported calculations in which the distorted waves were obtained numerically from a semiempirically determined distortion potential. Spin-orbit coupling effects were neglected in the target states and the sum of the DCS's for the "singlet" and "triplet" final states were calculated as a good approximation to the unresolved DCS. Their results are in reasonably good agreement with the unresolved $4s$, $4s'$ DCS's of Lewis *et al.*[6] The only other calculation which is available in the literature for the DCS for electron-impact excitation of the argon atom is that of Ganas and Green.[8] They used the Born approximation and consequently interference among the various partial waves was not properly described.

There have been more experimental and theoretical results reported for integral cross sections for excitation of various electronic states of Argon than for the DCS's. From an experimental standpoint, this is due to the relative ease by which apparent excitation (or photon emission cross sections) can be measured. From a theoretical viewpoint, this work has been motivated by the need for such data in modeling studies of a variety of discharge processes involving argon. The early experimental work on the electron-impact excitation of the resonance lines of argon by Fischer,[9] Herrmann,[10] Volkova and Devyatov,[11] and Zapesochnyi and Feltsan[12] has been well summarized by McConkey and Donaldson.[13] They also suggest that some of the early measurements may be in error and examine, in some detail, cascade contributions to the measured emission cross sections for the argon resonance lines. Mentall and Morgan[14] recently reported absolute emission cross sections at an electron energy of 200 eV for those emission features that lie between 70 and 110 nm. Schaper and Scheibner[15] have reported a measurement of the total excitation cross section with an improved Maier-Leibnitz apparatus, from the lowest excitation threshold to 16 eV. Absolute cross sections for excitation of the metastable states of argon have been reported by Borst[16] who also discussed the earlier measurements of Kuprianov[17] and of Lloyd *et al.*[18] In addition to the results reported by Sawada *et al.*[7] and by Ganas and Green,[8] theoretical integral cross sections for excitation of many of the discrete states of argon have been reported by Peterson and Allen,[19] and by Eggarter,[20] as determined from generalized oscillator strength relationships and the Bethe approximation.

In order to test quantitatively the original ideas of Massey and Mohr,[4] it is desirable to perform a calculation that incorporates distortion and exchange effects in *ab initio* way. The first-order many-body theory (FOMBT) of inelastic scattering [also called the random-phase approximation (RPA)], which was first introduced by Csanak *et al.*[21] contains these physical effects and has been applied to the electron impact excitation of various states of the helium atom.[22-25] The FOMBT can be considered to be one form of the DWA which incorporates static and exchange distortion effects on the free-electron wave functions and the inelastic T matrix consists of both direct and exchange parts. Consequently, it includes the physical effects that are believed to be the most important for describing inelastic scattering in the intermediate energy region (between about 30 eV and 100 eV incident electron energy). The FOMBT has been shown to be one of many possible forms of a DWA by Rescigno *et al.*[26] The relationship of the FOMBT to the more conventional forms of the DWA has also been discussed by Pindzola and Kelly,[27] by Calhoun *et al.*[28] by Madison,[29] by Winters,[30] and a comprehensive review has recently been given about these, and related methods, by Bransden and McDowell.[31] In the general context of the equation-of-motion (EOM) method, FOMBT, has also been reviewed by McCurdy *et al.*[32] A special feature of the FOMBT as a DWA is that the distorted waves for *both* the incident and scattered electrons are calculated in the field of the *ground state* of the target, including static and exchange distortion effects. This lowest-order approximation has the numerical advantage of making the continuum orbitals orthogonal to each other, although it appears as "unphysical" for the outgoing electron. A very similar form of the DWA has also been used by Madison and Shelton[33] in a calculation for the electron-impact excitation of the $2\,^1P$ state of helium for which various forms of the DWA have been compared numerically and the FOMBT form gave the best overall agreement with experiment. It is interesting to note that Sawada *et al.*[7] also used the same distortion potential for the incoming and scattered electrons. Progress has also recently been made in obtaining experimental DCS's for the excitation of argon. Tam and Brion[34] reported the first measurements of the relative DCS's for excitation of the resolved $4s[3/2]_2^0(^3P_2)$, $4s'[1/2]_0^0(^3P_0)$, and $4s'[1/2]_1^0(^1P_1)$ levels.

In the work reported here, the FOMBT has been applied (in a simplified form) for the calculation of the differential and integral cross sections for the electron-impact excitation of the $4s[3/2]_1^0(^3P_1)$, $4s[3/2]_2^0(^3P_2)$, $4s'[1/2]_0^0(^3P_0)$, and $4s'[1/2]_1^0(^1P_1)$ states of argon, for incident electron energies of 16, 20, 30, 50, and 80.4 eV. In order to calculate cross sections for the individual $J=1$ levels, the spin-orbit coupling effect in the excited-state wave functions must be included, since this effect is responsible for the splitting of the $J=1$ levels and the results reported here show that the shape of the DCS for the excitation of the $4s[3/2]_1^0(^3P_1)$ state is strongly influenced by spin-orbit coupling. The spin-orbit coupling effect in the target states has not been considered in any of the previous calculations of the DCS although the importance of various coupling schemes for the integral cross sections for electron-impact excitation of argon has been investigated by Veldre, Lyash, and Rabik[36] in the Born approximation. The results obtained in these calculations are compared with the recent experimental data of Chutjian and Cartwright[35] and with the earlier relative DCS measurements of Lewis *et al.*[6] for unresolved states. In most cases the agreement is good. The coherence properties of the $4s[3/2]_1^0(^3P_1)$ and $4s'[1/2]_1^0(^1P_1)$ states excited by electrons, predicted by the FOMBT, are being reported in a separate publication.

II. THEORETICAL FOUNDATION

The formulation of the FOMBT (or RPA) of electron-atom inelastic scattering was motivated by the observation that the *Bethe-Salpeter amplitude* plays the same role for inelastic scattering as the one-electron Green's function does in the many-body description of elastic scattering.[37]

A. Elastic scattering

The *one-electron Green's function*, $G(1,1')$, is defined by the formula[37-40] (atomic units are used throughout)

$$G(1,1')\equiv\frac{1}{i}\langle\Psi_0|\,T(\psi(1)\psi^\dagger(1'))\,|\Psi_0\rangle\,, \tag{1}$$

where $\psi(1)\equiv\psi(\vec{r}_1\sigma_1 t_1)$ is the electron-field operator in the Heisenberg representation, the symbol 1 denotes the combined spatial ($\vec{r}_1$), spin (σ_1), and time (t_1) coordinates of the electron labeled as number 1, $|\Psi_0\rangle$ refers to the ground-state wave vector of the target, and T is the Wick time-ordering operator. The *Bethe-Salpeter amplitude*,[40] $X_n(1,1')$, is defined as

$$X_n(1,1')\equiv\langle\Psi_n|\,T(\psi(1)\psi^\dagger(1'))\,|\Psi_0\rangle\,, \tag{2}$$

where $|\Psi_n\rangle$ refers to the excited-state wave vector of the target. In the case of elastic scattering, the importance of the one-electron Green's function was recognized by Bell and Squires[41] and by Namiki[42] and formed the foundation of the many-body description of that process. From the interpreta-

tion of the one-electron Green's function,[37,40-42] the S matrix for the elastic-scattering process can be written in terms of Eq. (1) as

$$S_{\tilde{k}',\tilde{k}} = i \lim_{t_1' \to +\infty,\, t_1 \to -\infty} \int dx_1' dx_1 \phi^*_{\tilde{k}'}(x_1', t_1') \times G(1',1)\phi_{\tilde{k}}(x_1, t_1), \quad (3)$$

where $\phi_{\tilde{k}}(x,t)$ denotes a propagating plane wave, $\tilde{k},\tilde{k}'$ refers to the quantum numbers (momentum *and* spin) of the incoming and outgoing electron, respectively, the limits are taken with "adiabatic decoupling,"[37] and the symbol x refers to the combined spatial ($\vec{r}$) and spin (σ) coordinates. In order to calculate the limit in Eq. (3), the *Dyson equation*[37,39] for $G(1,1')$,

$$G(1,1') = G_0(1,1') + \int d2d3 G_0(1,2)\sum(2,3)G(3,1') \quad (4)$$

is used. In Eq. (4), $G_0(1,1')$ is the *free-particle Green's function*, $\sum(2,3)$ is called the *irreducible self-energy*,[37,39] and the integration for particles 2 and 3 means integration over spatial and time coordinate and summation over spin. Substitution of Eq. (4) into Eq. (3) gives the following result for the S matrix for elastic scattering[43]

$$S_{\tilde{k}',\tilde{k}} = \delta(\epsilon_{\tilde{k}} - \epsilon_{\tilde{k}'})\left(\delta_{\tilde{k}',\tilde{k}} + \frac{1}{i}\int d2d3 \phi^*_{\tilde{k}}(2) \times \sum(2,3) f^{(+)}_{\tilde{k}}(3)\right). \quad (5)$$

In Eq. (5), the quantity $f^{(+)}_{\tilde{k}}(1)$, the *Feynman-Dyson amplitude*, has been introduced by using the formula[37]

$$f^{(+)}_{\tilde{k}}(1) = \lim_{t' \to -\infty} i \int dx' G(1,1')\phi_{\tilde{k}}(1'). \quad (6)$$

From Eqs. (4) and (6), the Dyson equation for this amplitude can be written as

$$f^{(+)}_{\tilde{k}}(1) = \phi_{\tilde{k}}(1) + \int G_0(1,2)\sum(2,3) f_{\tilde{k}}(3)\, d2d3. \quad (7)$$

Equations (5) and (7) together suggest that $f^{(+)}_{\tilde{k}}(1)$ can be interpreted[42] as the "effective one-electron orbital" of one electron moving in the field of the other electrons described by the nonlocal optical potential $\sum(2,3)$.

B. Inelastic scattering

In the case of *inelastic scattering*, the S matrix can be written in the form[21,37]

$$S_{n\tilde{q},0\tilde{p}} = \lim_{t_1' \to \infty,\, t_1 \to -\infty} \int dx_1 dx_1' \phi_{\tilde{p}}(x_1, t_1) \times X_n(1',1)\phi^*_{\tilde{q}}(x_1', t_1'), \quad (8)$$

where the subscript 0 refers to the initial (ground) state and n to the final (excited) state of the target. The quantities $\tilde{p}$ and $\tilde{q}$ refer to the quantum numbers (momentum and spin) of the incoming and outgoing electron, respectively. From a comparison of Eqs. (3) and (8), it is apparent that the quantity $X_n(1,1')$ plays the same role for inelastic scattering as the quantity $G(1,1')$ plays for elastic scattering, in order to evaluate the time limits in Eq. (8), an equation for $X_n(1,1')$ is needed. This equation is provided in the form of the *Bethe-Salpeter equation* as

$$X_n(1',1) = \int d3\, d3' d4\, d4' G(1',3)G(3',1) \times \Xi(3,4,3',4')X_n(4',4), \quad (9)$$

where the quantity $\Xi(34,3'4')$ is called the *two-point vertex function*.[37,40] Substituting Eq. (9) into (8), the following exact formula is obtained for the S *matrix for inelastic scattering*[21,44]:

$$S_{n\tilde{q},0\tilde{p}} = \frac{1}{i^2}\int d1\, d2\, d3\, d4 f^{(+)}_{\tilde{p}}(1) f^{(-)*}_{\tilde{q}}(2) \times \Xi(24,13)X_n(3,4). \quad (10)$$

From this *exact* formula, the FOMBT (or RPA) is obtained by substituting (i) the first-order approximation for the two-point vertex function[21]

$$\Xi^{\mathrm{RPA}}_{(34,3'4')} = i\delta(3-4')\delta(3'-4')V(3-3') - i\delta(3-3')\delta(4-4')V(3-4), \quad (11)$$

where

$$V(1-2) = \delta(t_1 - t_2)\frac{1}{|\vec{r}-\vec{r}_2|}, \quad (12)$$

and (ii) the Hartree-Fock approximation for the Feynman-Dyson orbitals.[45] By making those approximations in Eq. (10), and carrying-out the indicated time-integration[46] the following result is obtained for the S *matrix for inelastic scattering*:

$$S^{\mathrm{RPA}}_{0\tilde{p},n\tilde{q}} = -2\pi i\delta(\epsilon_{\tilde{p}} - \epsilon_{\tilde{q}} - \omega_n)T^{\mathrm{RPA}}_{0\tilde{p},n\tilde{q}} = -2\pi i\delta(\epsilon_{\tilde{p}} - \epsilon_{\tilde{q}} - \omega_n)\int dx_1 dx_2 f^{(-)*\mathrm{HF}}_{\tilde{q}}(x_1) f^{(+)\mathrm{HF}}_{\tilde{p}}(x_2) V_{on}(x_1,x_2), \quad (13)$$

where $\epsilon_{\tilde{p}}$ and $\epsilon_{\tilde{q}}$ refer to the energies of the incoming and outgoing electron, respectively, and ω_n to the excitation energy of the state n. $V^{\mathrm{RPA}}_{on}(x_1,x_2)$ is defined by the formula

$$V^{\mathrm{RPA}}_{on}(x_1,x_2) = \delta(x_1 - x_2)\int \frac{dx'}{|\vec{r}_1 - \vec{r}'|} X^{\mathrm{RPA}}_n(x',x') - \frac{1}{|\vec{r}_1 - \vec{r}_2|} X^{\mathrm{RPA}}_n(x_2,x_1), \quad (14)$$

where $X_n^{\mathrm{RPA}}(x_2,x_1)$ is the value of the transition density matrix[32] in the RPA between states n and 0, $\vec{r}_1$ and $\vec{r}_2$ are the spatial parts of x_1 and x_2, respectively, $\delta(x_1-x_2)\equiv\delta(\vec{r}_1-\vec{r}_2)\delta_{\sigma_1\sigma_2}$, where σ_1 and σ_2 are the spin parts of x_1 and x_2, respectively, and $\delta_{\sigma_1\sigma_2}$ is the Kronecker delta symbol. The transition density matrix can be defined by the formula[47]

$$X_n(x,x')=\langle\Psi_n|\psi^\dagger(x)\psi(x')|\Psi_0\rangle, \tag{15}$$

where $|\Psi_0\rangle$ and $|\Psi_n\rangle$ refer to the wave vectors of the ground and excited state, respectively, and $\psi(x)$ is the electron field operator in the Schrödinger representation.[37] The transition density matrix can be expressed in terms of the wave functions of the ground $[\Psi_0(x_1x_2\cdots x_n)]$ and excited $[\Psi_n(x_1x_2\cdots x_n)]$ states, respectively, in the form

$$X_n(x,x')=N\int\Psi_n^*(x,x_2\cdots x_N)\times\Psi_0(x',x_2\cdots x_N)dx_2\cdots dx_N, \tag{16}$$

where N refers to the number of electrons in the system. In Eq. (13) $f_{\vec{p}}^{(+)\mathrm{HF}}(x)$ and $f_{\vec{q}}^{(-)\mathrm{HF}}(x)$ are the electron scattering orbitals in the HF approximation with outgoing wave and incoming wave boundary conditions, respectively.

III. ANALYTICAL AND NUMERICAL DETAILS

A. Wave functions

In order to obtain realistic cross sections for electron impact excitation of the resolved states of argon, spin-orbit interaction has to be included in the description of the excited states of this system.[48] To be completely consistent, the spin-orbit interaction should be introduced into the total $(N+1)$ electron Hamiltonian, as, for example, was done in atomic spectroscopy by Condon and Shortley.[48] Following this procedure, spin-orbit coupling effects would enter the calculations of the $f_{\vec{p}}^{(+)\mathrm{HF}}(x)$, $f_{\vec{q}}^{(-)\mathrm{HF}}(x)$ orbitals as well as the transition density matrix $X_n^{\mathrm{RPA}}(x_1,x_2)$. However, the essential effects due to spin-orbit coupling in the target can be included and the scope of the calculations kept reasonably small by making the following two approximations.

(1) Spin-orbit coupling effects were neglected in the calculation of the $f_{\vec{p}}^{(+)\mathrm{HF}}(x)$ and $f_{\vec{q}}^{(-)\mathrm{HF}}(x)$ orbitals. These effects are expected to be important only if spin-polarization effects are to be calculated[49] but are believed to be negligible if spin orientations are averaged over. This is the usual case when the incident electrons are not spin polarized and the spin of the outgoing electron is not detected. This assumption makes it possible to factor the free-electron wave functions into the form

$$f_{\vec{p}}^{(+)\mathrm{HF}}(x)=f_{\vec{p}}^{(+)\mathrm{HF}}(\vec{r})\eta_{m_{s_1}}(\sigma), \tag{17}$$

$$f_{\vec{q}}^{(-)\mathrm{HF}}(x)=f_{\vec{q}}^{(-)\mathrm{HF}}(\vec{r})\eta_{m_{s_2}}(\sigma), \tag{18}$$

where $\vec{p}$ and $\vec{q}$ refer to the momentum and m_{s_1} and m_{s_2} to the spin projection of the incoming and outgoing electrons, respectively, and $\eta_{m_s}(\sigma)$ is the Pauli spin function.

(2) Spin-orbit effects were incorporated into the calculation for the transition density matrix by the following simplified scheme.[50] Spin-orbit coupling and electron correlation effects were *assumed* not to be important in the ground state of the argon atom, so that the Hartree-Fock (HF) approximation was adopted for Ψ_0, i.e.,

$$\Psi_0\approx\Psi_0^{\mathrm{HF}}=(1s)^2(2s)^2(2p)^6(3s)^2(3p)^6. \tag{19}$$

Here the customary symbols for spatial configuration[51] have been introduced to denote the properly normalized Slater determinant.

An approximate ground-state wave function of this form was first calculated by Hartree and Hartree[52] and was also used by Knox[53] to calculate optical oscillator strengths from the ground state to the $4s'[1/2]_1^0$ and $4s[3/2]_1^0$ states. It should also be mentioned that recent calculations of Swanson and Armstrong[54] show that ground-state correlation effects are important for rare-gas photoionization processes (i.e., optical transitions between ground and continuum states). Thon-That and Armstrong[55] have taken into consideration ground-state correlation effects in a Born calculation for the total cross section of electron-impact excitation of argon for the unresolved $4s$, $4s'$ levels and found it to be important. However, since the Born approximation was used, and spin-orbit interaction was not considered in the excited state, it is not possible to draw quantitative conclusions about the importance of ground-state correlation effects in electron-impact excitation of argon at intermediate energies. The importance of ground-state correlation effects in the FOMBT description of electron scattering by argon at intermediate energies will be considered in a future study.

For the excited-state wave functions, spin-orbit coupling has to be taken into consideration. In calculating the excited-state wave functions, a fixed-core HF approximation (FCHF) was used initially for the construction of the LS-coupled $[3p^5 4s]\ 4^1P$ configuration. (This configuration consists of states that are eigenstates of the $\hat{L}^2$, $\hat{S}^2$, $\hat{L}_z$, $\hat{S}_z$ operators with eigenvalues $L=1$, $S=0$, and $M_L=0,\pm1$, $M_S=0$.) The $(1s)^2(2s)^2(2p)^6(3p)^5$ core orbitals were chosen to be that of the HF ground state [i.e., the ones entering Eq. (19)]. The $4s$ orbital was obtained in the FCHF approximation for the $[(3p)^5 4s]\ 4^1P$ configuration, keeping the

core orbitals fixed.[56] The *same* 4s orbital was then used to construct the LS-coupled wave functions that belong to the $[(3p)^5 4s]\ ^4P$ configuration.[57] (These wave functions are also eigenfunctions of the $\hat{L}^2$, $\hat{S}^2$, $\hat{L}_z$, and $\hat{S}_z$ operators with $L=1$, $S=1$, and $M_L=\pm 1, 0$ eigenvalues.) Since the spin-orbit coupling effects are known to be most important for the description of excited states of argon[48,49] the wave functions belonging to the $[(3p)^5 4s]\ 4^1P$ and $[(3p)^5 4s]\ 4^3P$ LS-coupled configurations were recoupled into $J=0,1,2$ states where J refers to the eigenvalue of the *total* angular momentum operator. First a transformation using Clebsh-Gordan coefficients was effected which resulted in states that are eigenfunctions of the $\hat{L}^2$, $\hat{S}^2$, $\hat{J}^2$, and $\hat{J}_z$ operators. These states can be grouped into the configurations: $[(3p)^5 4s]4^1P_1$; $[(3p)^5 4s]4^3P_1$; $[(3p)^5 4s]4^3P_0$ and $[(3p)^5 4s]4^3P_2$ where the subindex refers to the J value and every configuration represents a collection of states with $M_J = J, J-1, \ldots, -J$. Spin-orbit coupling was then introduced into the states with $J=1$ by the semiempirical method of Cowan and Andrew[58] and Cowan.[59] Thus, the wave functions belonging to the $4s'[3/2]_1^0$ and $4s[1/2]_1^0$ levels were obtained as a linear combination of those that belong to the $[(3p)^5 4s]4^1P_1$ and $[(3p)^5 4s]4^3P_1$ configurations in the form

$$|4s'[1/2]_1^0; M_J\rangle = b\,|[(3p)^5 4s]4^1P_1; M_J\rangle + a\,|[(3p)^5 4s]4^3P_1; M_J\rangle, \quad (20a)$$

$$|4s[3/2]_1^0; M_J\rangle = -a\,|[(3p)^5 4s]4^1P_1; M_J\rangle + b\,|[(3p)^5 4s]4^3P_1; M_J\rangle, \quad (20b)$$

where $a=-0.450$, $b=0.893$, and the wave function is now characterized by the term symbol or configuration symbol and the M_J value referring to the eigenvalue of the J_z operator. The coefficients (a and b) were determined from the experimentally observed energy levels of the 4s and 4s′ states. It is to be noted that states with different J or M_J value do not couple by spin-orbit interaction since the spin-orbit coupling operator commutes with the $\hat{J}^2$ and $\hat{J}_z$ operators. Thus the $|[(3p)^5 4s]4^3P_0; M_J=0\rangle$ and $|[(3p)^5 4s]4^3P_2; M_J\rangle$ wave vectors do not change due to spin-orbit interaction, thus we can write

$$|4s[3/2]_2^0; M_J\rangle = |[(3p)^5 4s]4^3P_2; M_J\rangle, \quad (21a)$$

$$|4s'[1/2]_0^0; M_J=0\rangle = |[(3p)^5 4s]4^3P_0; M_J=0\rangle. \quad (21b)$$

B. Transition density matrices

Now that approximations have been introduced for the ground- and excited-state wave functions, Eqs. (19)–(21) can be used in Eq. (16) for the calculation of the transition density matrix for the states discussed. The results can be summarized in the following form.

For the $J=1$ states, we obtain

$$X_{0,4s'[1/2]_1^0,M_J}(x_1,x_2) = bX_{0,4s^1P_1,M_J}(x_1,x_2) + aX_{0,4s^3P_1,M_J}(x_1,x_2), \quad (22a)$$

$$X_{0,4s[3/2]_1^0,M_J}(x_1,x_2) = -aX_{0,4s^1P_1,M_J}(x_1,x_2) + bX_{0,4s^3P_1,M_J}(x_1,x_2), \quad (22b)$$

and for the $J=0$ and 2 states,

$$X_{0,4s'[1/2]_1^0,M_{J=0}}(x_1,x_2) = X_{0,4s^3P_0,M_{J=0}}(x_1,x_2) \quad (23a)$$

and

$$X_{0,4s[3/2]_1^0,M_J}(x_1,x_2) = X_{0,4s^3P_2,M_J}(x_1,x_2). \quad (23b)$$

In Eqs. (21a)–(23b), the following notation was introduced:

$$X_{0,4s}2S+1_{L_J,M_J}(x_1,x_2) = \langle [(3p)^5 4s]4^{2S+1}L_J; M_J\,|\psi^\dagger(x_1)\psi(x_2)|\psi_0\rangle. \quad (24)$$

As discussed in the preceding section the $|[(3p)^5 4s]4^{2S+1}L_J; M_J\rangle$ state vectors were obtained from the $|[(3p)^5 4s]4^{2S+1}L; M_L, M_S\rangle$ state vectors via a Clebsch-Gordan transformation,

$$|[(3p)^5 4s]4^{2S+1}L_J; M_J\rangle = \sum_{M_L M_S} \langle LM_L SM_S\,|\,LSJM_J\rangle\,|[(3p)^5 4s]4^{2S+1}L; M_L M_S\rangle, \quad (25)$$

where the $|[(3p)^5 4s]4^{2S+1}L; M_L M_S\rangle$ wave vectors are the ones that belong to the $[(3p)^5 4s]4^{2S+1}L$ configuration with M_L and M_S eigenvalues of the $\hat{L}_z$ and $\hat{S}_z$ operators. Combining Eqs. (24) and (25), the transition density matrix for the $|[(3p)^5 4s]4^{2S+1}L_J; M_J\rangle$ states can be written as

$$X_{0,4s}2S+1_{L_J;M_J}(x_1,x_2) = \sum_{M_L M_S} \langle LM_L SM_S\,|\,LSJM_J\rangle X_{0,4s}2S+1_{L;M_L,M_S}(x_1,x_2), \quad (26)$$

where

$$X_{0,4s}2S+1_{L'M_{L'},M_S}(x_1,x_2) = \langle [(3p)^5 4s]4^{2S+1}L; M_L M_S\,|\,\psi^\dagger(x_1)\psi(x_2)\,|\Psi_0^{\mathrm{HF}}\rangle. \quad (27)$$

The simplest way to calculate (in practice) this latter transition density matrix is to use the technique

introduced by Altick and Glassgold[47(a)] to generate excited-state wave vectors. In their formulation, we can write

$$|(3p)^5 4s^{2S+1}L; M_L M_S\rangle = C^+(LM_L, SM_S\{4s3p\})|\Psi_0^{\mathrm{HF}}\rangle , \tag{28}$$

where we have defined

$$C^+(LM_L, SM_S\{i\,\alpha\}) = e^{i(\pi/2)} \sum_{m_\alpha, \mu_\alpha} (-1)^{m_\alpha+\mu_\alpha} (l_\alpha - m_\alpha l_i m_i | l_\alpha l_i LM) \left(\tfrac{1}{2} - \mu_\alpha \tfrac{1}{2} \mu_i | \tfrac{1}{2} S M_S\right) a_i^\dagger a_\alpha ; \tag{29}$$

here i refers to all quantum numbers $n_i l_i m_i \frac{1}{2} \mu_i$ of the one-electron orbitals $\phi_{n_i l_k m_i (1/2)\mu_i}(\vec{r}, \sigma)$ that has been selected as reference. In our case the one-electron orbitals are selected as the ground-state HF orbitals and the FCHF excited-state orbitals of ^1P symmetry. In Eq. (29) i refers to an excited state, α to a ground-state orbital and $a_i^\dagger, a_\alpha$ are the second quantized creation and annihilation operators that are related to the field operator $\psi(r)$ by the following equation:

$$\psi(r) = \sum_i a_i \phi_i(r) + \sum_\alpha a_\alpha \phi_\alpha(r) . \tag{30}$$

The use of Eq. (28), (29), and the commutation properties of the a_i and a_α second-quantization operators allows rapid calculation of the transition density matrices, given by Eq. (27). The final result can be given in the form

$$X_{0,\,4s}{}^{2S+1}{}_{P;M_L,M_S}(x_1, x_2) = X_{3p\to 4s,\,L,M_L}(\vec{r}_1, \vec{r}_2)\zeta_{S,M_S}(\sigma_1, \sigma_2), \quad (S = 0, 1) \tag{31a}$$

where

$$X_{3p\to 4s,\,S,M_L}(\vec{r}_1, \vec{r}_2) = R_{3p}(r_2) R_{4s}(r_1) Y_{1M_L}(\hat{r}_1) Y_{00}(\hat{r}_2), \tag{31b}$$

where the $\phi_{3p1M_L}(\hat{r})$ normalized HF ground-state orbital was factored into the form

$$\phi_{3p1M_L}(\vec{r}) = R_{3p}(r) Y_{1M_L}(\hat{r}) \tag{31c}$$

and the normalized 4s orbital was written as

$$\phi_{4s}(\vec{r}) = R_{4s}(r) Y_{00}(\hat{r}) . \tag{31d}$$

In the above formulas $Y_{LM}(\hat{r})$ denotes the spherical harmonics as defined by Edmonds.[60] The $\zeta_{S,M_S}(\sigma_1\sigma_2)$ spin functions are defined as follows:

$$\zeta_{0,0}(\sigma_1\sigma_2) = \frac{1}{\sqrt{2}} [\alpha(\sigma_1)\alpha^*(\sigma_2) + \beta(\sigma_1)\beta^*(\sigma_2)] , \tag{32a}$$

$$\zeta_{1,0}(\sigma_1\sigma_2) = \frac{1}{\sqrt{2}} [\alpha(\sigma_1)\alpha^*(\sigma_2) - \beta(\sigma_1)\beta^*(\sigma_2)] , \tag{32b}$$

$$\zeta_{1,-1}(\sigma_1\sigma_2) = -\alpha(\sigma_1)\beta^*(\sigma_2) , \tag{32c}$$

$$\zeta_{1,+1}(\sigma_1\sigma_2) = \beta(\sigma_1)\alpha^*(\sigma_2) . \tag{32d}$$

Substituting Eqs. (31a)–(31d) and (32a)–(32d) into Eq. (26) and the results into Eqs. (22a) and (22b) and (23a) and (22b), one obtains expressions for the spin-orbit coupled transition density matrices in terms of the 4s and 3p orbitals and spin functions.

C. Cross-section formulas

Substituting these transition densities in Eq. (14), to be used in Eq. (13), the T matrix can be obtained in the FOMBT (with the additional simplifications introduced) for the excitation of each particular $4s[j]^0_J, M_J$ state (where $j = \frac{1}{2}, \frac{3}{2}$ and $J = 0, 1, 2$; $M_J = -J, -J+1, \ldots, J$) which will be denoted by

$$T_{0,\vec{p}m_{s_1};4s[j]^0_J,M_J,\vec{q}m_{s_2}} ,$$

and the S matrix is related to the T matrix by the usual definition $S = 1 - T$. From the T matrices, the differential cross section for the excitation of a particular $4s[j]^0_J$ *level* can be obtained (the term level here refers to the collection of all the M_J states for a given J). Since the incident electrons are not usually spin polarized and the spin of the outgoing electron has not been detected in the experiments reported to date, an averaging for the spin of the incident electron and a sum for the spin of the outgoing electrons (as well as the magnetic sublevel of the final target state) has to be introduced. The DCS for excitation of a given level then takes the following form:

$$\left(\frac{d\sigma}{d\Omega}\right)_{4s[j]^0_J} = \frac{q}{4\pi^2 p} \sum_{M_J} \frac{1}{2} \sum_{m_{s_1}, m_{s_2}} |T_{0,\vec{p}m_{s_1};4s[j]^0_J,M_J,\vec{q}m_{s_2}}|^2 , \tag{33}$$

where p and q refers to the magnitude of the $\vec{p}$ and $\vec{q}$ vectors, respectively, i.e., $p = |\vec{p}|, q = |\vec{q}|$. Using the result obtained above for T matrices in Eq. (33) the following formulas are obtained for the various level cross sections.

$$\left(\frac{d\sigma}{d\Omega}\right)_{4s'[1/2]_2^0} = \frac{1}{4\pi^2}\frac{q}{p}\left[\frac{b^2}{2}\left(\left|2T^D_{L,M_L=1,S=0} - T^E_{L,M_L=1,S=0}\right|^2 + \left|2T^D_{L,M_L=0,S=0} - T^E_{L,M_L=0,S=0}\right|^2 + \left|2T^D_{L,M_L=-1,S=0} - T^E_{L,M_L=-1,S=0}\right|^2\right) + \frac{a^2}{2}\left(\left|T^E_{L,M_L=0,S=1}\right|^2 + \left|T^E_{L,M_L=1,S=1}\right|^2 + \left|T^E_{L,M_L=-1,S=1}\right|^2\right)\right], \tag{34a}$$

$$\left(\frac{d\sigma}{d\Omega}\right)_{4s[3/2]_1^0} = \frac{1}{4\pi^2}\frac{q}{p}\left[\frac{a^2}{2}\left(\left|2T^D_{L,M_L=1,S=0} - T^E_{L,M_L=1,S=0}\right|^2 + \left|2T^D_{L,M_L=0,S=0} - T^E_{L,M_L=0,S=0}\right|^2 + \left|2T^D_{L,M_L=-1,S=0} - T^E_{L,M_L=-1,S=0}\right|^2\right) + \frac{b^2}{2}\left(\left|T^E_{T,M_L=0,S=1}\right|^2 + \left|T^E_{L,M_L=1,S=1}\right|^2 + \left|T^E_{L,M_L=-1,S=1}\right|^2\right)\right], \tag{34b}$$

$$\left(\frac{d\sigma}{d\Omega}\right)_{4s'[1/2]_0^0} = \frac{1}{4\pi^2}\frac{q}{p}\frac{1}{6}\left(\left|T^E_{L,M_L=1,S=1}\right|^2 + \left|T^E_{L,M_L=0,S=1}\right|^2 + \left|T^E_{L,M_L=0,S=1}\right|^2\right), \tag{34c}$$

$$\left(\frac{d\sigma}{d\Omega}\right)_{4s[3/2]_2^0} = \frac{1}{4\pi^2}\frac{q}{p}\frac{5}{6}\left(\left|T^E_{L,M_L=1,S=1}\right|^2 + \left|T^E_{L,M_L=0,S=1}\right|^2 + \left|T^D_{L,M_L=1,S=1}\right|^2\right), \tag{34d}$$

where $T^D_{L,M_L,S}$ and $T^E_{L,M_L,S}$ are defined by the following expression:

$$T^D_{L,M_L,S} = \int d\vec{r}_1 d\vec{r}_2 f^{(+)\mathrm{HF}}_{\vec{p}}(\vec{r}_1) f^{(-)\mathrm{HF}*}_{q}(\vec{r}_1) V(\vec{r}_1 - \vec{r}_2) X_{3p\to 4s,S}(\vec{r}_2, \vec{r}_2) \tag{35a}$$

and

$$T^E_{L,M_L,S} = \int d\vec{r}_1 d\vec{r}_2 f^{(+)\mathrm{HF}}_{\vec{p}}(\vec{r}_1) f^{(-)\mathrm{HF}*}_{\vec{q}}(\vec{r}_2) V(\vec{r}_1 - \vec{r}_2) X_{3p\to 4s,S}(\vec{r}_2, \vec{r}_1). \tag{35b}$$

Thus the calculation of the DCS's according to (34a)–(34d) reduces to the calculation of $T^D_{L,M_L,S}$ and $T^E_{L,M_L,S}$ integrals given by (35a) and (35b), respectively. It can be noted that, in our approximation scheme,

$$\left(\frac{d\sigma}{d\Omega}\right)_{4s[3/2]_2^0} = 5\left(\frac{d\sigma}{d\Omega}\right)_{4s'[1/2]_0^0}.$$

D. Angular momentum analysis

In order to calculate the three-dimensional integrals indicated in (35a) and (35b), an angular momentum expansion is introduced for $f^{\mathrm{HF}(+)}_{\vec{p}}(\vec{r})$ and $f^{\mathrm{HF}(-)}_{\vec{p}}(\vec{r})$. The z axis can be chosen along the $\vec{p}$ vector (momentum of incident electron) and consequently the expansion for $f^{(+)\mathrm{HF}}_{\vec{p}}(\vec{r})$ can be written in the following form:

$$f^{(+)\mathrm{HF}}_{\vec{p}}(\vec{r}) = \sum_{l=0}^{\infty} \frac{2l+1}{pr} i^l \cos\delta^{\mathrm{HF}}_l(p) e^{i\delta^{\mathrm{HF}}_l(p)} u^{\mathrm{HF}}_l(p,r) P_l(\cos\theta), \tag{36}$$

where $u^{\mathrm{HF}}_l(p,r)$ is the HF continuum radial function with the asymptotic form,

$$u^{\mathrm{HF}}_l(p,r) \underset{r\to\infty}{\longrightarrow} \sin\left(pr - \frac{l\pi}{2}\right) + \tan\delta^{\mathrm{HF}}_l \cos\left(pr - \frac{l\pi}{2}\right), \tag{37}$$

where δ^{HF}_l is the lth partial wave HF phase shift, θ is the polar angle of $\vec{r}$, and $P_l(\cos\theta)$ is the lth order Legendre polynomial.[61] The angular momentum expansion for $f^{(-)\mathrm{HF}}_{\vec{q}}(\vec{r})$ can be given in the following form:

$$f^{(-)\mathrm{HF}}_{\vec{q}}(\vec{r}) = \frac{4\pi}{qr}\sum_{l=0}^{\infty}\sum_{m=-l}^{+l} i^l \cos\delta^{\mathrm{HF}}_l(q) e^{-i\delta^{\mathrm{HF}}_l(q)} u^{\mathrm{HF}}_l(q,r) Y^*_{l,m}(\hat{q}) Y_{l,m}(\hat{r}), \tag{38}$$

where $\hat{q}$ refers to the polar angles of the vector $\vec{q}$. Substituting expansions (36), (38), and the formula given by Eq. (31b) into (35a) and (35b), respectively, along with the usual multipole expansion for $V(\vec{r}_1 - \vec{r}_2)$, the following result is obtained:

$$T^{D}_{LM_L S}=\frac{4\pi}{pq}\sum_{l''\geq|M_L|}\sum_{l'=|l''-1|}^{l''+1}\frac{(-1)^{(l'+1-l'')/2}}{\sqrt{3}}(-i)\exp\{i[\delta^{\mathrm{HF}}_{l'}(p)+\delta^{\mathrm{HF}}_{l''}(q)]\}$$
$$\times(2l'+1)(2l''+1)\left(\frac{(l''-M_L)!}{(l''+M_L)!}\right)^{1/2}\begin{bmatrix} l' & l'' & 1\\ 0 & 0 & 0\end{bmatrix}\begin{bmatrix} l' & l'' & 1\\ 0 & -M_L & M_L\end{bmatrix}$$
$$\times\cos\delta^{\mathrm{HF}}_{l'}(p)\cos\delta^{\mathrm{HF}}_{l''}(q)I^{p,q}_{l',l'',S}P^{M_L}_{l''}(\cos\theta_q)e^{-iM_L\phi_q} \tag{39}$$
$$\equiv\sum_{l''}T^{D}_{l''}P^{M_L}_{l''}(\cos\theta_q)e^{-iM_L\phi_q},$$

where

$$I^{p,q}_{l',l'',S}\equiv\int_0^\infty dr_1\int_0^\infty dr_2 u^{\mathrm{HF}*}_{l'}(q,r_1)u^{\mathrm{HF}}_{l''}(p,r_1)\frac{r_<}{r_>^2}P_{3p}(r_2)P_{4s}(r_2) \tag{40}$$

and

$$T^{E}_{L,M_L,S}=\frac{4\pi}{pq}\sum_{l''\geq|M_L|}\sum_{l'=l''-1}^{l''+1}(-1)^{(l'+l''+1)/2}(-i)\sqrt{3}\,(2l''+1)$$
$$\times\exp\{i[\delta^{\mathrm{HF}}_{l'}(p)+\delta^{\mathrm{HF}}_{l''}(q)]\}\cos\delta^{\mathrm{HF}}_{l'}(p)\cos\delta^{\mathrm{HF}}_{l''}(q)\left(\frac{(l''-M_L)!}{(l''+M_L)!}\right)$$
$$\times\begin{bmatrix} l'' & l' & 1\\ 0 & 0 & 0\end{bmatrix}\begin{bmatrix} l'' & l' & 1\\ M_L & 0 & -M_L\end{bmatrix}P^{M_L}_{l''}(\cos\theta_q)e^{-iM_L\phi_q}J^{pq}_{l'l''S}$$
$$\equiv\sum_{l''\geq|M_L|}T^{E}_{l'}P^{M_L}_{l''}(\cos\theta_q)e^{-iM_L\phi_q}, \tag{41}$$

where

$$J^{pq}_{l'l''S}\equiv\int_0^\infty dr_1\int_0^\infty dr_2 u^{\mathrm{HF}*}_{l'}(q,r_2)u^{\mathrm{HF}}_{l'}(p,r_1)\frac{r_<^{l'}}{r_>^{l'+1}}P_{3p}(r_2)P_{4s}(r_1). \tag{42}$$

E. Numerical implementation

In its numerical implementation, the sums over l' in Eq. (39) and (41) have to be terminated at a finite value, $l_{\max}$. However, in the case of $T^{D}_{L,M_L,S}$ the series for l' is slowly converging and $l_{\max}$ has to be chosen quite large ($l_{\max}>90$). This numerical difficulty can be overcome if $T^{D}_{L,M_L S}$ is written in the rearranged form[7]

$$T^{D}_{L,M_L S}=\sum_{l''}T^{D}_{l''}P^{M_L}_{l''}(\cos\theta_q)e^{-iM_L\phi_q}+T^{\mathrm{Born}}_{L,M_L S}-\sum_{l''}T^{\mathrm{Born}}_{l''}P^{M_L}_{l''}(\cos\theta_q)e^{-iM_L\phi_q}, \tag{43}$$

where $T^{\mathrm{Born}}_{L,M_L,S}$ is obtained from $T^{D}_{L,M_L,S}$ by the substitution $f^{\mathrm{HF}(+)}_{\vec{p}}(\vec{r})\to e^{i\vec{p}\cdot\vec{r}}$, $f^{\mathrm{HF}(-)}_{\vec{q}}(\vec{r})\to e^{-i\vec{q}\cdot\vec{r}}$ (which implies in Eq. (36) the substitution $\delta^{\mathrm{HF}}_l\to 0, u^{\mathrm{HF}}_l(p,r)\to pr j_l(pr)$ [$j_l(x)$ is the lth order spherical Bessel function]). $T^{\mathrm{Born}}_{L,M_L,S}$ can be calculated without partial-wave analysis using the following formula:

$$T^{\mathrm{Born}}_{L,M_L S}=\frac{(4\pi)^{3/2}}{K^2}iY^*_{LM_L}(\theta_K,\phi_K)I_L(K), \tag{44}$$

where $\vec{K}=\vec{p}-\vec{q}$ is the momentum-transfer vector, $K=|\vec{K}|$, and θ_K,ϕ_K are the polar angles of $\vec{K}$ and $I_L(K)$ is the one-dimensional integral

$$I_L(K)=\int_0^\infty P_{3p}(r_2)P_{4s}(r_2)j_L(Kr_2)dr_2. \tag{45}$$

Using the substitutions mentioned above $T^{\mathrm{Born}}_{l''}$ can be obtained from Eq. (39);

$$T^{\mathrm{Born}}_{l''}\equiv 4\pi\sum_{l'=|l''-1|}^{l''+1}\frac{(-1)^{(l'+1-l'')/2}}{\sqrt{3}}(-i)(2l'+1)(2l''+1)\left(\frac{(l''-M_L)!}{(l''+M_L)!}\right)^{1/2}$$
$$\times\int dr_1\int dr_2 r_1 r_2 j_{l'}(qr_1)j_{l''}(pr_1)\frac{r_<}{r_>^2}P_{3p}(r_2)P_{4s}(r_2). \tag{46}$$

In Eq. (43) the sum over l'' in the first and third term can be terminated at some $l''=\bar{l}_{\max}$ value where $\delta_l^{\mathrm{HF}}\approx 0$ and $u_{l''}^{\mathrm{HF}}(p,r)\approx j_{l''}(p,r)$ approximations hold. This usually appears at a much smaller value of $\bar{l}_{\max}$ then the value $l_{\max}$ needed to reach the convergence in the series given by Eq. (39). In this case the formula given by Eq. (43) ensures that undistorted partial waves $[u_l(p,r)\to prj_l(p,r);\ \delta_l^{\mathrm{HF}}\to 0]$ are taken into consideration up to infinite order for any value of $\bar{l}_{\max}$.

Another numerical problem arises in calculating the individual integrals $I^{pq}_{l'l''S}$. These integrals can be written in the form [33]

$$I^{pq}_{l'l''}=\int_0^\infty dr_1 u_{l'}^{\mathrm{HF}*}(q,r_1)u_{l''}^{\mathrm{HF}}(p,r_1)V_{3p\to 4s}(r_1)\,, \quad (47)$$

where

$$V_{3p\to 4s}(r)=\int_0^\infty dr_2 \frac{r_<}{r_>^2}P_{3p}(r_2)P_{4s}(r_2)\,. \quad (48)$$

From the definition of $V_{3p\to 4s}(r)$ it immediately follows that

$$V_{3p\to 4s}(r)\underset{r\to\infty}{\longrightarrow}\frac{D_{3p\to 4s}}{r^2}\,, \quad (49)$$

where

$$D_{3p\to 4s}=\int_0^\infty dr\, r P_{3p}(r)P_{4s}(r)\,. \quad (50)$$

This means that $V_{3p\to 4s}(r)$ is of long-range nature and the integral in Eq. (48) has to be extended to very large values of r. The numerical calculation of $I^{pq}_{l'l''S}$ can be simplified however in view of the fact, that (i) $V_{3p\to 4s}(r)$ reaches its asymptotic value indicated in Eq. (49) outside the range of the orbital $4s$ (ii) in the intermediate-low energy region, $u_l^{\mathrm{HF}}(p,r)$ reaches its asymptotic form [given by Eq. (37)] for values of r ($r<100$ a.u.). Thus the integration region in Eq. (47), for r_1, was divided into two parts,

$$I^{pq}_{l'l''}=\int_0^{R_0} dr_1 u_{l'}^{\mathrm{HF}*}(q,r_1)u_{l''}^{\mathrm{HF}}(p,r_1)V_{3p\to 4s}(r_1)$$
$$+\int_{R_0}^\infty dr_1 u_{l'}^{\mathrm{HF}*}(q,r_1)u_{l''}^{\mathrm{HF}}(p,r_1)V_{3p\to 4s}(r_1)\,. \quad (51)$$

In the first term ($[0,R_0]$ interval), accurate numerical integration is used, whereas in the second term (in the $[R_0,\infty]$ interval), the $u_l^{\mathrm{HF}}(q,r)$, $u_{l''}^{\mathrm{HF}}(p,r)$, and $V_{3p\to 4s}(r)$ are *all* approximated by their asymptotic forms as given by Eqs. (37) and (49). If l' and l'' are not very large ($l',l''\leq 15$), R_0 can be conveniently chosen $R_0\approx 70$–130 a.u.

IV. RESULTS AND DISCUSSION

The results from the FOMBT description of the electron-impact excitation of the argon atom, that can be compared with experiment (or other theory), are the integral and differential cross sections (DCS's) for excitation of the four electronic states considered in this study, and the parameters characterizing the electron-photon coincidence measurements involving the two $J=1$ states. The differential and integral cross sections predicted by the FOMBT will be compared with the results from other theoretical models and the available experimental data in this paper and the description of the electron-photon coincidence parameters for argon will be discussed in subsequent publications.[62]

A. Differential cross section

1. Spin-orbit coupling in the target

Before embarking on a detailed comparison of the present theoretical results with the available experimental data, the role of spin-orbit coupling in the target should be elucidated. As described in Section III A above, relativistic effects were not included in the dynamics of the scattering process but only in the description of the *final* target state. Figure 1(b) illustrates the importance of spin-orbit coupling in the final target state for a proper description of the excitation of the $^3P_1$ state. The effect is particularly dramatic for scattering angles less than 60 degrees since the transition is optically forbidden in LS coupling. As a consequence of a small admixture (~20%) of the ^1P wave function into the ^3P wave function, the shape of the DCS is transformed into one characteristic of an optically allowed transition and in excellent agreement with the experimental magnitude and shape. On the other hand, the effect of the spin-orbit coupling on the $^1P_1$ DCS is essentially negligible as shown in Fig. 1(a). As will be apparent in the next section, the effect of spin-orbit coupling on the DCS for excitation of the $^3P_1$ and $^1P_1$ states is the same as shown in Fig. 1 at all incident electron energies examined in this study. It was not necessary to consider relativistic effects on the $^3P_{0,2}$ states since there are no other $n=4$ states with the same J values.

The Born DCS for excitation of the ^1P state is also shown in Fig. 1(a) for comparison with the FOMBT result. It is obvious from the comparison in Fig. 1(a) that the Born description of the excitation process is inadequate and both electron distortion and exchange effects need to be included to properly describe the excitation process.

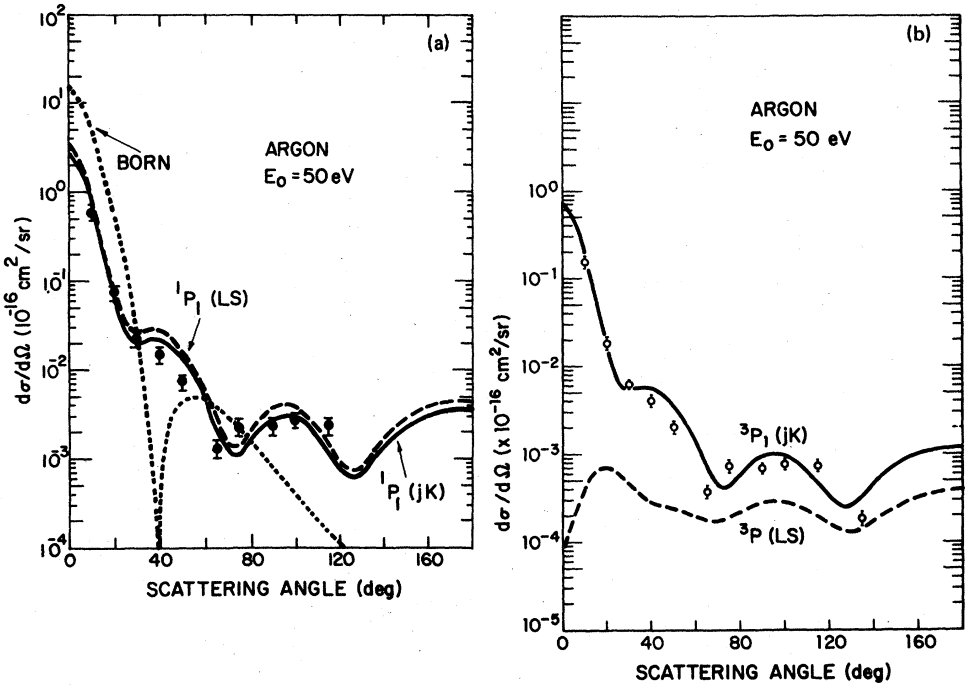

FIG. 1. Differential cross section (DCS) for excitation of $^1P_1$ and $^3P_1$ states of argon at 50 eV, with and without spin-orbit coupling; (a) excitation of $^1P_1$; (b) excitation of $^3P_1$. The short dashed line in (a) is the Born result. The solid line is for spin-orbit (jK) coupling. The dashed line is for LS coupling.

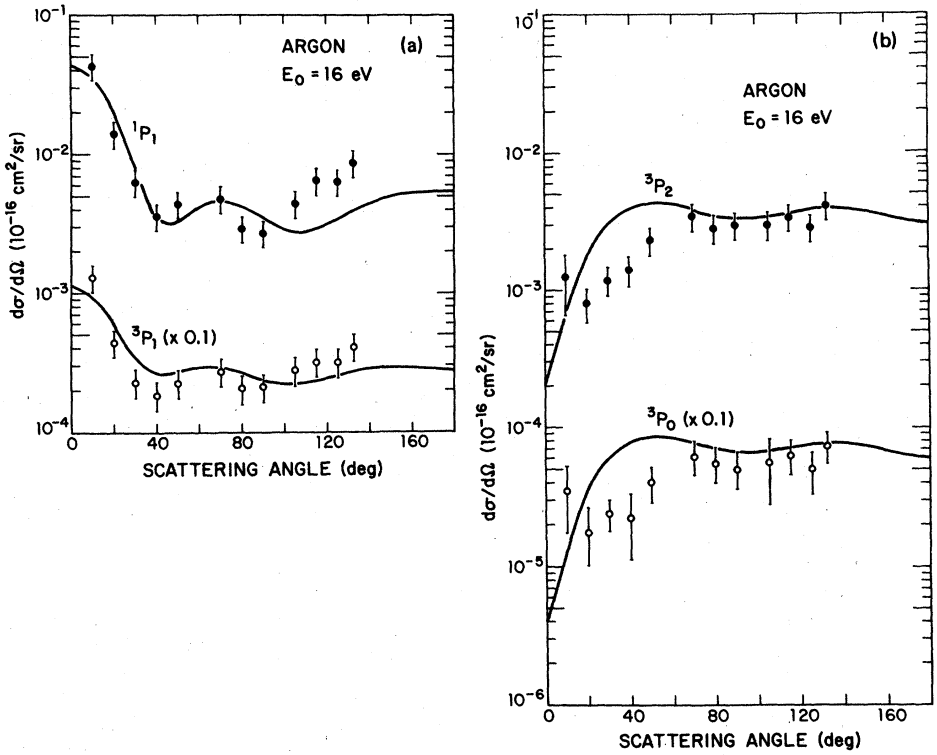

FIG. 2. DCS for excitation of the (a) $^1P_1$ and $^3P_1$ and the (b) $^3P_2$ and $^3P_0$ states of argon at 16-eV incident electron energy. The solid lines are the results from the FOMBT and the data points are the results from electron energy-loss measurements (Ref. 35). Note that the results for $^3P_1$ and $^3P_0$ have been *reduced* by a factor of 10.

TABLE I. Differential, integral (σ_I), and inelastic momentum-transfer (σ_M) cross sections (in 10^{-16} cm^2/sr and 10^{-16} cm^2) for electron-impact excitation of the $^3P_0$ and $^1P_1$ states of argon obtained using the FOMBT.

Incident energy (eV)										
Final state	16		20		30		50		80.4	
Angle (deg)	$^3P_0$	$^1P_1$	$^3P_0$	$^1P_1$	$^3P_0$	$^1P_1$	$^3P_0$	$^1P_1$	$^3P_0$	$^1P_1$
(0)	0.3812 – 4 [a]	0.4338 – 1	0.1013 – 2	0.2105 + 0	0.1954 – 2	0.7220 + 0	0.2365 – 4	0.2765 + 1	0.4922 – 4	0.6088 + 1
10	0.1284 – 3	0.3599 – 1	0.1227 – 2	0.1583 + 0	0.2191 – 2	0.3913 + 0	0.1439 – 3	0.6966 + 0	0.1346 – 3	0.5857 + 0
20	0.3530 – 3	0.2074 – 1	0.1694 – 2	0.7230 – 1	0.2515 – 2	0.1051 + 0	0.2368 – 3	0.6571 – 1	0.1169 – 3	0.3215 – 1
30	0.6059 – 3	0.8702 – 2	0.2070 – 2	0.2371 – 1	0.2388 – 2	0.3391 – 1	0.1588 – 3	0.2038 – 1	0.3384 – 4	0.1299 – 1
40	0.7904 – 3	0.3674 – 2	0.2153 – 2	0.9781 – 2	0.1835 – 2	0.2359 – 1	0.9847 – 4	0.2157 – 1	0.1521 – 4	0.7457 – 2
50	0.8667 – 3	0.3295 – 2	0.1973 – 2	0.9740 – 2	0.1212 – 2	0.1834 – 1	0.8236 – 4	0.1332 – 1	0.9949 – 5	0.2694 – 2
60	0.8514 – 3	0.4231 – 2	0.1655 – 2	0.1153 – 1	0.7472 – 3	0.1248 – 1	0.6588 – 4	0.4737 – 2	0.6000 – 5	0.8021 – 3
70	0.7883 – 3	0.4665 – 2	0.1303 – 2	0.9551 – 2	0.4778 – 3	0.8530 – 2	0.5978 – 4	0.1215 – 2	0.5921 – 5	0.6987 – 3
80	0.7200 – 3	0.4292 – 2	0.9865 – 3	0.9712 – 2	0.3538 – 3	0.6548 – 2	0.7518 – 4	0.1702 – 2	0.6906 – 5	0.1161 – 2
90	0.6761 – 3	0.3548 – 2	0.7550 – 3	0.7457 – 2	0.3080 – 3	0.5251 – 2	0.9535 – 4	0.2953 – 2	0.7500 – 5	0.1549 – 2
100	0.6705 – 3	0.2957 – 2	0.6500 – 3	0.5832 – 2	0.2892 – 3	0.4056 – 2	0.9647 – 4	0.2927 – 2	0.7694 – 5	0.1516 – 2
110	0.7001 – 3	0.2820 – 2	0.6901 – 3	0.5411 – 2	0.2836 – 3	0.3324 – 2	0.7741 – 4	0.1803 – 2	0.8943 – 5	0.1101 – 2
120	0.7464 – 3	0.3157 – 2	0.8538 – 3	0.6130 – 2	0.3069 – 3	0.3725 – 2	0.5461 – 4	0.8008 – 3	0.9603 – 5	0.5538 – 3
130	0.7821 – 3	0.3788 – 2	0.1081 – 2	0.7456 – 2	0.3744 – 3	0.5304 – 2	0.4512 – 4	0.6920 – 3	0.9202 – 5	0.1815 – 2
140	0.7850 – 3	0.4471 – 2	0.1298 – 2	0.8717 – 2	0.4854 – 3	0.7154 – 2	0.5760 – 4	0.1368 – 2	0.8643 – 5	0.3940 – 3
150	0.7503 – 3	0.5014 – 2	0.1450 – 2	0.9454 – 2	0.6233 – 3	0.8261 – 2	0.8397 – 4	0.2280 – 2	0.9372 – 5	0.1007 – 2
160	0.6938 – 3	0.5343 – 2	0.1525 – 2	0.9614 – 2	0.7567 – 3	0.8367 – 2	0.1090 – 3	0.3010 – 2	0.1195 – 4	0.2396 – 2
170	0.6431 – 3	0.5491 – 2	0.1546 – 2	0.9475 – 2	0.8507 – 3	0.7948 – 2	0.1263 – 3	0.3445 – 2	0.1477 – 4	0.2523 – 2
180	0.6229 – 3	0.5529 – 2	0.1548 – 2	0.9380 – 2	0.8839 – 3	0.7699 – 2	0.1328 – 3	0.3590 – 2	0.1626 – 4	0.2903 – 2
σ_I	0.009 08	0.0642	0.015 73	0.1700	0.009 29	0.2414	0.001 08	0.2723	0.000 19	0.2477
σ_M	0.009 16	0.0569	0.014 52	0.1273	0.006 79	0.1208	0.000 98	0.0661	0.000 12	0.0361

[a] The notation 0.3812 – 4 means 0.3812×10^{-4}.

TABLE II. Same as Table I except for excitation of the $^3P_2$ and $^3P_1$ states of argon.

Incident energy (eV)	16		20		30		50		80.4	
Final state	$^3P_2$	$^3P_1$	$^3P_2$	$^3P_1$	$^3P_2$	$^3P_1$	$^3P_2$	$^3P_1$	$^3P_2$	$^3P_1$
Angle (deg)										
0	0.1906 – 3 [a]	0.1110 – 1	0.5063 – 2	0.5572 – 1	0.9772 – 2	0.1877 + 0	0.1183 – 3	0.7023 + 0	0.2461 – 3	0.1546 + 1
10	0.6420 – 3	0.9425 – 2	0.6137 – 2	0.4295 – 1	0.1096 – 1	0.1043 + 0	0.7195 – 3	0.1772 + 0	0.6728 – 3	0.1490 + 0
20	0.1765 – 2	0.6056 – 2	0.8472 – 2	0.2215 – 1	0.1258 – 1	0.3231 – 1	0.1184 – 2	0.1722 – 1	0.5845 – 3	0.8425 – 2
30	0.3029 – 2	0.3566 – 2	0.1035 – 1	0.1065 – 1	0.1194 – 1	0.1396 – 1	0.7940 – 3	0.5532 – 2	0.1692 – 3	0.3375 – 2
40	0.3952 – 2	0.2702 – 2	0.1077 – 1	0.7303 – 2	0.9176 – 2	0.1010 – 1	0.4924 – 3	0.5697 – 2	0.7605 – 4	0.1928 – 2
50	0.4333 – 2	0.2776 – 2	0.9867 – 2	0.6890 – 2	0.6058 – 2	0.7369 – 2	0.4118 – 3	0.3568 – 2	0.4974 – 4	0.7063 – 3
60	0.4257 – 2	0.2980 – 2	0.8272 – 2	0.6631 – 2	0.3736 – 2	0.4840 – 2	0.3294 – 3	0.1350 – 2	0.3000 – 4	0.2171 – 3
70	0.3942 – 2	0.2949 – 2	0.6516 – 2	0.5342 – 2	0.2389 – 2	0.3235 – 2	0.2990 – 3	0.4424 – 3	0.2961 – 4	0.1907 – 3
80	0.3600 – 2	0.2701 – 2	0.4933 – 2	0.4674 – 2	0.1769 – 2	0.2455 – 2	0.3759 – 3	0.6003 – 3	0.3453 – 4	0.3101 – 3
90	0.3381 – 2	0.2414 – 2	0.3775 – 2	0.3583 – 2	0.1540 – 2	0.2023 – 2	0.4767 – 3	0.9632 – 3	0.3750 – 4	0.4101 – 3
100	0.3352 – 2	0.2252 – 2	0.3250 – 2	0.2936 – 2	0.1446 – 2	0.1677 – 2	0.4824 – 3	0.9593 – 3	0.3847 – 4	0.4022 – 3
110	0.3501 – 2	0.2283 – 2	0.3450 – 2	0.2918 – 2	0.1418 – 2	0.1479 – 2	0.3870 – 3	0.6310 – 3	0.4471 – 4	0.2997 – 3
120	0.3732 – 2	0.2472 – 2	0.4269 – 2	0.3468 – 2	0.1534 – 2	0.1633 – 2	0.2730 – 3	0.3256 – 3	0.4802 – 4	0.1621 – 3
130	0.3911 – 2	0.2712 – 2	0.5406 – 2	0.4313 – 2	0.1872 – 2	0.2185 – 2	0.2256 – 3	0.2767 – 3	0.4601 – 4	0.4816 – 3
140	0.3925 – 2	0.2892 – 2	0.6489 – 2	0.5118 – 2	0.2427 – 2	0.2903 – 2	0.2881 – 3	0.4763 – 3	0.4322 – 4	0.1194 – 3
150	0.3751 – 2	0.2952 – 2	0.7251 – 2	0.5646 – 2	0.3117 – 2	0.3493 – 2	0.4198 – 3	0.7669 – 3	0.4686 – 4	0.2768 – 3
160	0.3469 – 2	0.2910 – 2	0.7626 – 2	0.5855 – 2	0.3783 – 2	0.3818 – 2	0.5452 – 3	0.1008 – 2	0.5974 – 4	0.6351 – 3
170	0.3216 – 2	0.2834 – 2	0.7731 – 2	0.5867 – 2	0.4253 – 2	0.3922 – 2	0.6313 – 3	0.1157 – 2	0.7387 – 4	0.6738 – 3
180	0.3115 – 2	0.2798 – 2	0.7740 – 2	0.5846 – 2	0.4419 – 2	0.3933 – 2	0.6638 – 3	0.1209 – 2	0.8131 – 4	0.7736 – 3
σ_I	0.0454	0.0366	0.0787	0.0784	0.0464	0.0819	0.005 40	0.0715	0.009 4	0.063 8
σ_M	0.0458	0.0349	0.0726	0.0647	0.0339	0.0457	0.004 88	0.0188	0.000 61	0.009 36

[a]The notation 0.1906 – 3 means 0.1906 $\times 10^{-3}$.

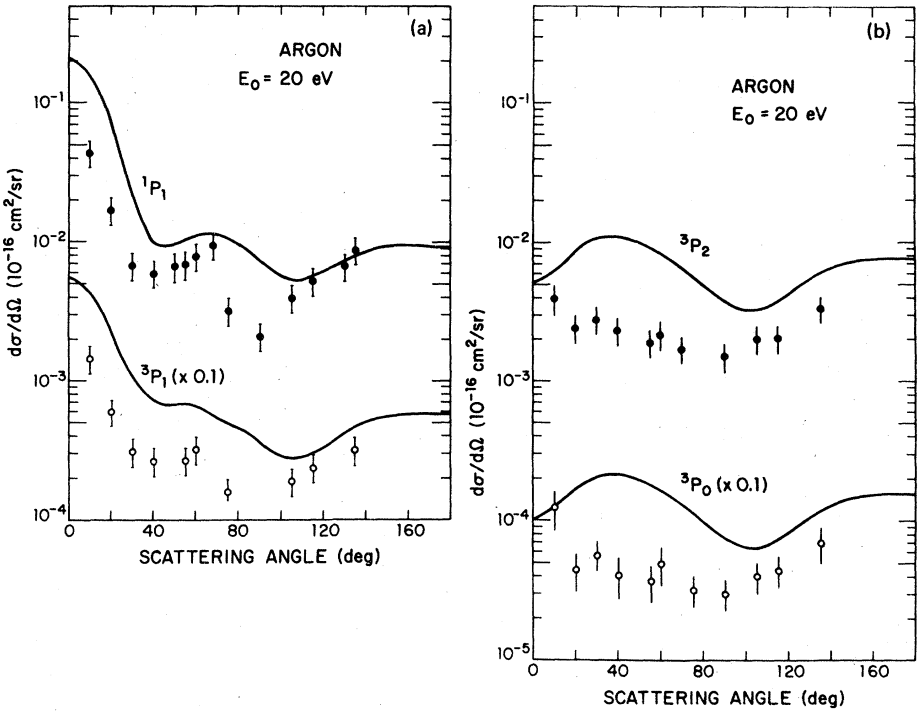

FIG. 3. Same as for Fig. 2 except for 20-eV incident electron energy. Note that the results for $^3P_1$ and $^3P_0$ have been *reduced* by a factor of 10.

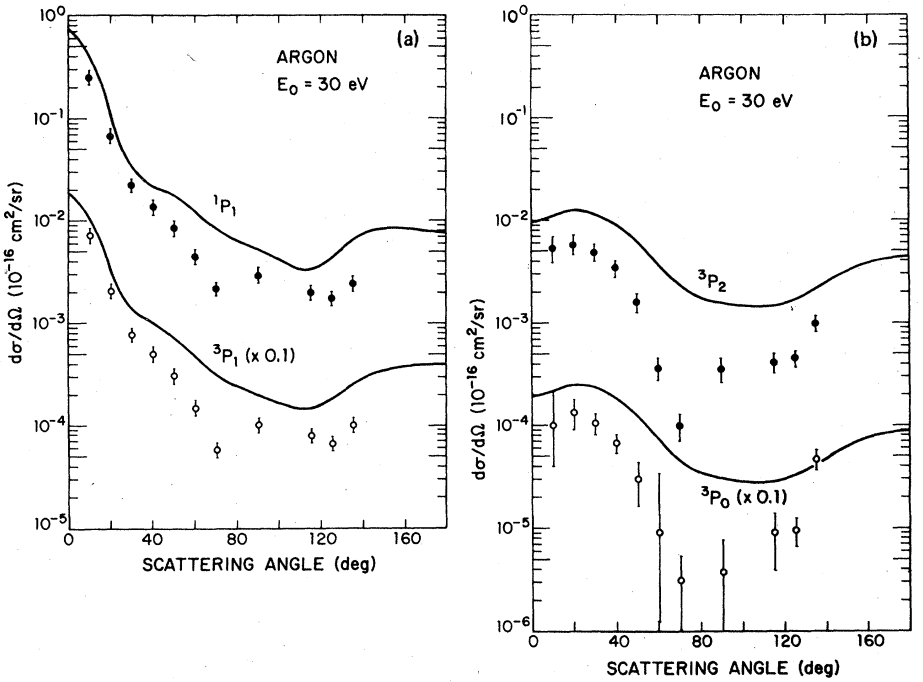

FIG. 4. Same as for Fig. 2 except for 30-eV incident electron energy. Note that the results for $^3P_1$ and $^3P_0$ have been *reduced* by a factor of 10.

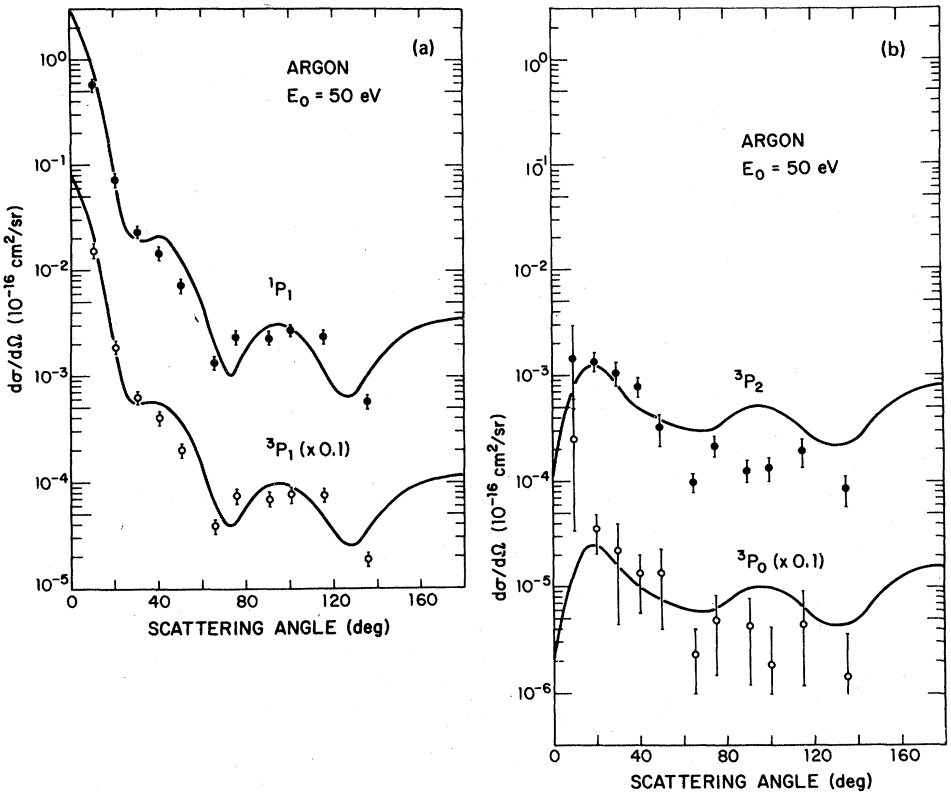

FIG. 5. Same as for Fig. 2 except for 50-eV incident electron energy. Note that the results for $^3P_1$ and $^3P_0$ have been *reduced* by a factor of 10.

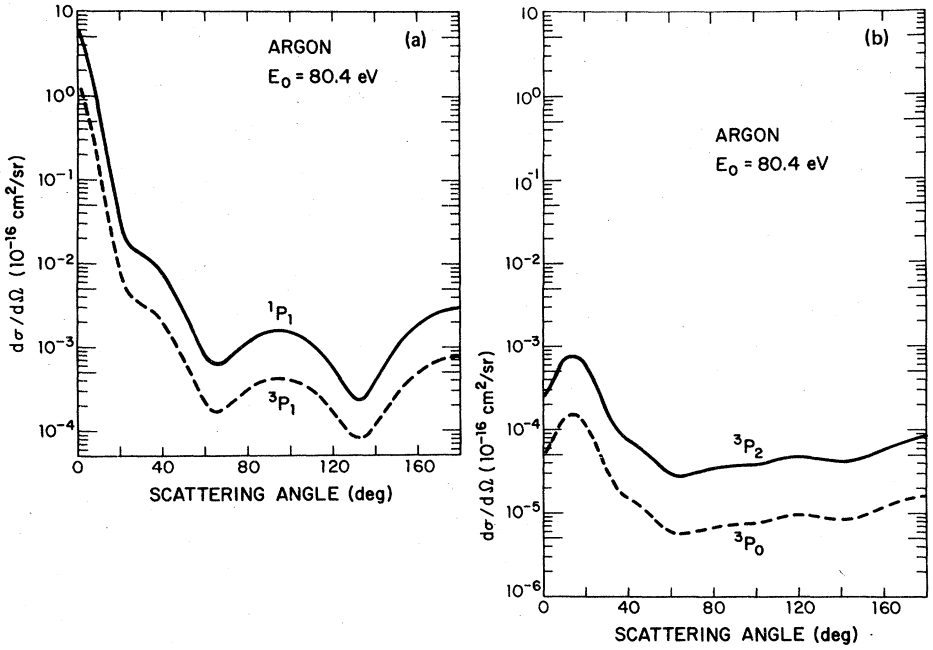

FIG. 6. DCS's for excitation of the $^1P_1$, $^3P_1$, $^3P_2$, and $^3P_0$ states of argon for an incident electron energy of 80.4 eV. There are no experimental data or other theoretical results on individual states for comparison. See Fig. 7.

2. *Comparison with experiment*

Tables I and II contain the FOMBT DCS values for excitation of the $^1P_1$, $^3P_1$, $^3P_2$, and $^3P_0$ states of argon at incident electron energies of 16, 20, 30, 50, and 80.4 eV. Figures 2–5 show comparisons of the theoretical DCS's with the absolute cross sections obtained[35] from electron energy-loss measurements. Figure 6 illustrates the results for an incident electron energy of 80.4 eV, for which no state specific experimental or theoretical results are currently available for comparison. Figures 2–5 show that the FOMBT results are qualitatively accurate at all incident energies considered and quantitatively accurate at 16 and 50 eV. When in error, the FOMBT appears to slightly overestimate the DCS. Generally speaking, the FOMBT appears to do a somewhat better job describing the optically allowed ($\Delta J = 1$) excitation processes than the optically forbidden ($^3P_2$, $^3P_0$) excitations. This can perhaps be understood on the qualitative grounds that excitation of the $^3P_2$ and $^3P_0$ states from the $^1S_0$ ground state of argon is dominated by exchange interactions which are not as well described by the FOMBT as the direct interactions that dominate the $^3P_1$ and $^1P_1$ excitations. This explanation is consistent with the observation that the DCS's for excitation of the $^3P_2$ and $^3P_0$ agree best with experiment at 50 eV incident electron energy and, at the higher incident energies, the nonlocal interactions (e.g., exchange) are relatively weaker than for the lower incident energies.

Figure 7 contains a comparison of the FOMBT results and the *relative* DCS measurements of Lewis *et al.*[6] for excitation of the unresolved 4*s* and 4*s*′ states. The theoretical DCS's for excitation of the $^3P_1$, $^1P_1$, $^3P_2$, and $^3P_0$ states were simply added together and the relative experimental DCS was normalized to the theoretical result at a scattering angle of 40 degrees. The shape of this composite theoretical DCS is seen to be in excellent agreement with the experimental result.

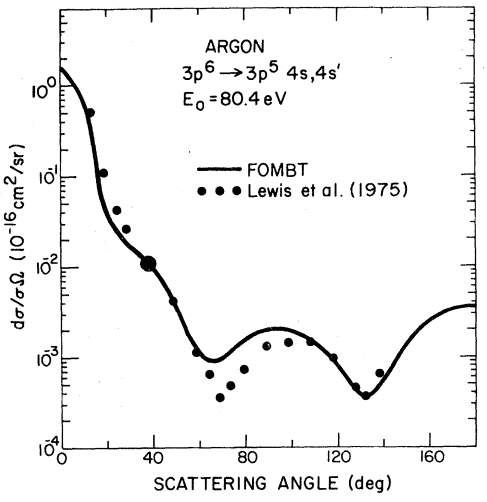

FIG. 7. DCS for excitation of the 4*s*, 4*s*′ manifold ($^1P_1 + ^3P_1 + ^3P_2 + ^3P_0$) for an incident electron energy of 80.4 eV. The solid line is the FOMBT result and the dots denote the relative results of Lewis *et al.* (Ref. 6) normalized to the theoretical DCS at a scattering angle of 40 degrees.

B. Integral cross sections

This section contains a comparison of the integral cross sections obtained in the FOMBT with the other theoretical and experimental results. Although it is known[63] that integral cross sections are a much less sensitive test of a theory than the DCS's, such a comparison is informative because the integral cross sections for inelastic scattering are the most frequently used in applications. Upper limits to integral cross sections can also be obtained experimentally by optical emission studies which provide additional data for comparison of the theoretical integral cross sections.

Figure 8 shows a comparison of the FOMBT integral cross section for excitation of the $^3P_0$ state with the same cross section deduced[35] from electron energy-loss measurements. The theoretical and experimental results are in good agreement except at 100 eV where the experimental value is substantially greater than theory. Figure 9 contains a comparison of the FOMBT integral cross section for excitation of the $^3P_2$ state with the cross section extracted[35] from electron energy-loss data. The experimental and theoretical results are in excellent agreement through-

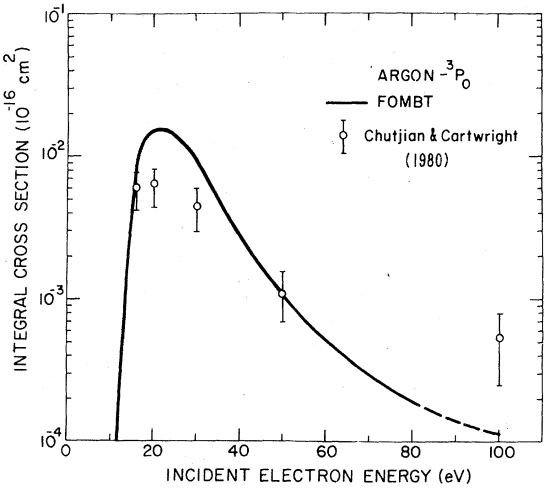

FIG. 8. Integral cross section for excitation of the $^3P_0$ state of argon. The solid line denotes the result from the FOMBT and the data points are the results from electron energy-loss measurements (Ref. 35).

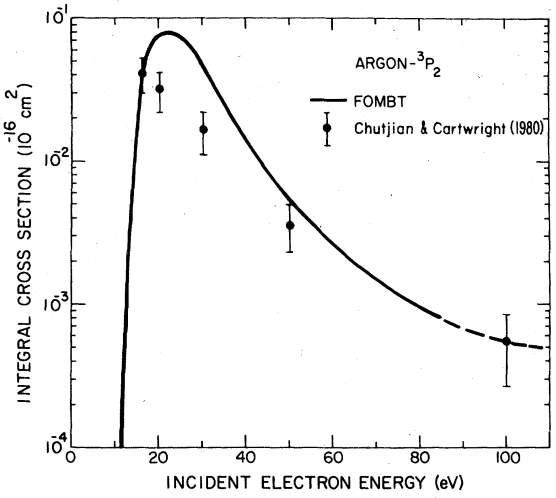

FIG. 9. Integral cross section for excitation of the $^3P_2$ state of argon. The solid line denotes the result from FOMBT and the data points are the results from electron energy-loss measurements (Ref. 35).

out the energy range except in the 20–50 eV where the theoretical cross section is somewhat large. There are no other measurements of the integral cross sections for excitation of the $^3P_0$ and $^3P_2$ states of argon for comparison.

Figure 10 contains a comparison of the FOMBT integral cross section for excitation of the $^1P_1$ with available experimental and other theoretical results. The FOMBT integral cross section agrees in shape and the energy location of the maximum value but is somewhat larger than the cross section deduced from electron energy-loss data,[35] which is the only measurement of the direct excitation cross section. Two different optical emission cross sections have been reported. McConkey and Donaldson[13] have reported a cross section for which most of the optical cascading from higher electronic states has been subtracted and their integral cross section agrees reasonably well in magnitude with the FOMBT result but has a different shape. Mental and Morgan[14] have recently reported an optical emission cross section that has no correction for cascade. As expected, their cross section is substantially larger than that reported by McConkey and Donaldson,[13] as well as the result obtained from electron energy-loss data. One other theoretical result has been reported, the results of a Born calculation by Peterson and Allen.[19] As expected, this integral cross section is larger than the FOMBT cross section and appears to asymptotically approach the FOMBT result as the incident electron energy increase.

Figure 11 contains a comparison of the FOMBT integral cross section for excitation of the $^3P_1$ state of argon to experimental measurements and the results of a Born calculation. The Born integral cross section is in good agreement with the FOMBT result over the entire energy range. Both of these theoretical cross sections are slightly larger but in reasonably good agreement with

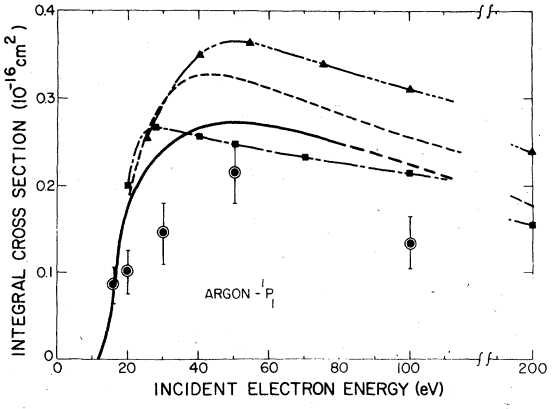

FIG. 10. Integral cross section for excitation of the $^1P_1$ state of argon. The heavy solid curve denotes the result of the FOMBT and the large data points with error bars are the results from electron energy-loss measurements (Ref. 35). Other results shown are the optical emission cross section of McConkey and Donaldson (Ref. 13) (squares) and of Mentall and Morgan (Ref. 14) (triangles), and the theoretical (first Born) results of Peterson and Allen (Ref. 19) (dashed line). See text for details.

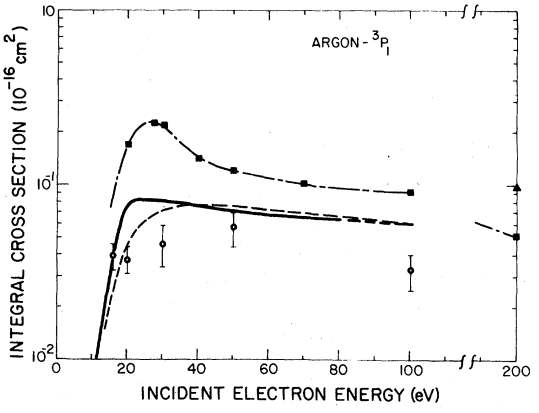

FIG. 11. Integral cross section for excitation of the $^3P_1$ state of argon. The heavy line denotes the result of the FOMBT and the data points with error bars are the results from electron energy-loss measurements (Ref. 35). Other results shown are the optical emission cross sections of McConkey and Donaldson (Ref. 13) (squares) and of Mentall and Morgan (Ref. 14) (triangle, 200 eV), and the theoretical (first Born) results of Peterson and Allen (Ref. 19) (dashed line). See text for details.

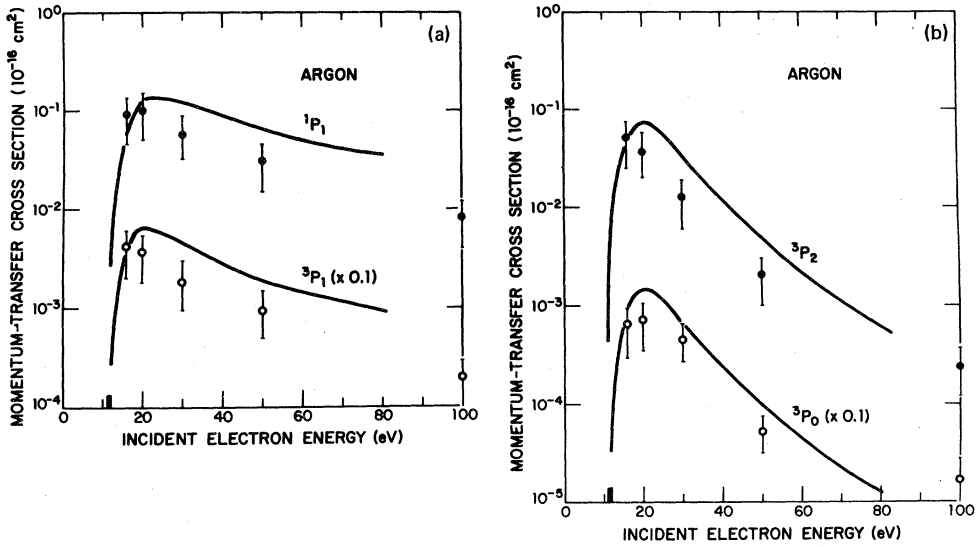

FIG. 12. Inelastic momentum-transfer cross sections associated with excitation of (a) $^1P_1$ and $^3P_1$, and (b) $^3P_2$ and $^3P_0$ states of argon. The heavy solid lines denote the results from the FOMBT and the data points with error bars are results from electron energy-loss measurements (Ref. 35). Note that the experimental and theoretical results for both the $^3P_1$ and $^3P_0$ excitations have been *reduced* a factor of 10 for clarity in plotting.

the results from electron energy-loss data.[35] Because of cascade contributions, the optical emission cross section of the McConkey and Donaldson[13] is larger than the other integral cross sections over the entire energy range.

C. Inelastic momentum transfer

The inelastic momentum-transfer cross section associated with electron-impact excitation of state i, $Q_i^m(E)$, is determined from the DCS according to[64]

$$Q_i^m(E)=\int_0^\pi (1-\lambda_i\cos\theta)\frac{d\sigma_i}{d\Omega}(\theta,p)d\Omega\,, \tag{52}$$

where

$$\lambda_i=(1-\Delta E_i/p^2)^{1/2}\,, \tag{53}$$

ΔE_i is the excitation energy of state i, and the other quantities are as defined above. As is evident from Eq. (48), Q_i^m is determined primarily by the DCS near $\theta=180°$. The difficulty in comparing theory and experiment for this quantity is that there are no direct measurements of the DCS's for scattering angles greater than 140°. The experimentally determined DCS's were extrapolated[35] smoothly from 140° to 180° but there is, of course, uncertainty associated with such a procedure.

Figure 12 contains a comparison of the inelastic momentum transfer associated with the excitation of the $^3P_0$, $^3P_2$, $^3P_1$, and $^1P_1$ states of argon, as calculated using FOMBT and as determined from analysis of the electron energy-loss data.[35] The FOMBT results are in semiquantitative agreement with the experimental data for all four transitions.

ACKNOWLEDGMENTS

The authors gratefully acknowledge the joint support of the US-Latin American Cooperative Science Program; NSF (OIP) and CNPq (Brazil) which made this research possible. We also express our appreciation to Dr. R. Cowan of Los Alamos Scientific Laboratory for providing the spin-orbit coupling wave functions used in these calculations and to Professor T. N. Chang of USC for help in checking certain of our radial integrals.

*Present address: Joint Institute for Laboratory Astrophysics, University of Colorado, Boulder, Colorado 80309.

†Present address: Barnes Engineering Co., 30 Commerce Road, Stamford, Conn. 06904.

[1]C. Brau, in *Excimer Lasers*, Topics in Applied Physics, edited by C. K. Rhodes, 30, 87 (Springer, Berlin, 1979).

[2]F. H. Nicoll and C. B. O. Mohr, Proc. R. Soc. London Ser. A 142, 320 (1933).

[3]The notation of C. E. Moore, *Atomic Energy Levels* (National Bureau of Standards, Circular No. 467, U. S.

Government Printing Office, Washington, D. C., 1948), Vol. 1 will be used putting J as subindex. The same notation was used also by B. H. Bransden and M. R. C. McDowell [Phys. Rep. 46, 249 (1978)]. The term notation in parenthesis refers to the closest approximation in a LS-coupled scheme.

[4]H. S. W. Massey and C. B. O. Mohr, Proc. R. Soc. London Ser. A 146, 880 (1934).

[5]N. F. Mott and H. S. W. Massey, *The Theory of Atomic Collisions*, 3rd edition (Oxford University Press, Oxford, 1965).

[6]B. R. Lewis, E. Weigold, and P. J. O. Teubner, J. Phys. B 8, 212 (1975).

[7]T. Sawada, J. E. Purcell, and A. E. S. Green, Phys. Rev. A 4, 193 (1971).

[8]P. S. Ganas and A. E. S. Green, Phys. Rev. A 4, 182 (1971).

[9]O. Fischer, Z. Phys. 86, 646 (1933).

[10]O. Herrmann, Ann. Phys. (N. Y.) 5, 143 (1936).

[11]L. M. Volkova and A. M. Devyatov, Opt. Spectrosc. (USSR) 7, 819 (1959) [Opt. Spectrosc. 7, 480 (1959)].

[12]I. P. Zapesochnyi and P. V. Feltsan, Opt. Spectrosc. (USSR) 20, 520 (1966) [Opt. Spectrosc. 20, 291 (1966)].

[13]J. W. McConkey and F. G. Donaldson, Can. J. Phys. 51, 914 (1973).

[14]J. E. Mentall and H. D. Morgan, Phys. Rev. A 14, 954 (1976).

[15]M. Schaper and H. Scheibner, Beitr. Plasmaphys. 9, 45 (1969).

[16]W. L. Borst, Phys. Rev. A 9, 1195 (1974).

[17]S. E. Kuprianov, Opt. Spectrosc. (USSR) 20, 85 (1966) [Opt. Spectrosc. 20, 163 (1966)].

[18]C. R. Lloyd, E. Weigold, P. J. O. Teubner, and S. T. Hood, J. Phys. B 5, 1712 (1972).

[19]L. R. Peterson and J. E. Allen, J. Chem. Phys. 56, 6068 (1972).

[20]E. Eggarter, J. Chem. Phys. 62, 833 (1975).

[21]Gy. Csanak, H. S. Taylor, and R. Yaris, Phys. Rev. A 3, 1322 (1971).

[22]L. D. Thomas, Gy. Csanak, H. S. Taylor, and B. S. Yarlagadda, J. Phys. B 7, 1719 (1974).

[23]A. Chutjian and L. D. Thomas, Phys. Rev. A 11, 1583 (1975).

[24]H. S. Taylor, A. Chutjian, and L. D. Thomas, in *Electron and Photon Interaction with Atoms*, edited by H. Kleinpoppen and M. R. C. McDowell (Plenum, New York, 1975), pp. 435–444.

[25]G. D. Meneses, N. T. Padial, and Gy. Csanak, J. Phys. B 11, L237 (1978).

[26]T. N. Rescigno, C. W. McCurdy, and V. McKoy, J. Phys. B 7, 2396 (1974).

[27]M. S. Pindzola and H. P. Kelly, Phys. Rev. A 11, 221 (1975).

[28]R. V. Calhoun, D. H. Madison, and W. N. Shelton, Phys. Rev. A 14, 1380 (1976).

[29]D. H. Madison, J. Phys. B 12, 3399 (1979).

[30]K. H. Winters, J. Phys. B 11, 149 (1978).

[31]B. H. Bransden and M. R. C. McDowell, Phys. Rep. 30C, 207 (1977).

[32]C. W. McCurdy, Jr., T. N. Rescigno, D. L. Yeager, and V. McKoy, in *Methods in Theoretical Chemistry*, edited by H. F. Schaefer III (Plenum, New York, 1977), Vol. 3.

[33]D. H. Madison and W. N. Shelton, Phys. Rev. A 7, 499 (1973).

[34]W.-C. Tam and C. E. Brion, J. Electron Spectrosc. Relat. Phenom. 2, 111 (1973).

[35]A. Chutjian and D. C. Cartwright, Phys. Rev. A 23, 2178 (1981) (preceding paper).

[36]V. Ya. Veldre, A. V. Lyash, and L. L. Rabik, in *Atomic Collisions III*, edited by V. Ya. Veldre (Akad. Nauk. Latv. SSR Inst. Fiz., Riga, 1965), p. 85.

[37]Gy. Csanak, H. S. Taylor, and R. Yaris, Adv. At. Mol. Phys. 7, 287 (1971).

[38]S. Raimes, *Many-Electron Theory* (North-Holland, Amsterdam, 1972).

[39]A. A. Abrikosov, L. P. Gor'kov, and I. Ye. Dzyaloshinskii, *Quantum Field Theoretical Methods in Statistical Physics*, 2nd edition, (Pergamon, New York, 1965).

[40]A. B. Migdal, *Theory of Finite Fermi Systems*, (Wiley, New York, 1967).

[41]J. S. Bell and E. J. Squires, Phys. Rev. Lett. 3, 96 (1959); J. S. Bell, in *Lectures on Many-Body Problems*, edited by E. R. Caianiello (Academic, New York, (1962).

[42]M. Namiki, Prog. Theor. Phys. (Kyoto) 23, 629 (1960); T. Kato, T. Kobayashi, and M. Namiki, Prog. Theor. Phys. (Kyoto) Suppl. 15, 3 (1969).

[43]R. T. Pu and E. S. Chang, Phys. Rev. 151, 31 (1966); H. P. Kelly, Phys. Rev. 160, 44 (1967); *ibid.*, 171, 54 (1968); M. Knowles and M. R. C. McDowell, J. Phys. B 6, 300 (1963); M. Ya. Amus'ya, N. A. Cherepkov, L. V. Chernysheva, S. G. Shaprio, and Tanchich, Zh. Eksp. Teor. Fiz. 68, 2023 (1975) [Sov. Phys.—JETP 41, 1012 (1976)].

[44]This exact formula has also been obtained by K. Emrich, Nucl. Phys. A 160, 1 (1971).

[45]This approximation is also called in scattering theory as the static-exchange approximation. The HF scattering orbitals are also frequently referred to as virtual orbitals.

[46]It has to be noted that Ref. 21 gives the scattering matrix in the generalized RPA (GRPA) [Eq. (46) of Ref. 21] which should be multiplied by a factor of 2π. The RPA form is obtained in the first iteration of the GRPA when the Feymann-Dyson orbitals $[f_p^{\mathrm{HF}}(r)]$ are used in the HF approximation. The RPA has been given in a more transparent form by Gy. Csanak, H. S. Taylor, and D. N. Tripathy, J. Phys. B 6, 2040 (1973) [Eq. (6) and (14)].

[47]The RPA for the transition density matrix has been discussed for atomic and molecular systems by (a) P. L. Altick and A. E. Glassgold, Phys. Rev. 133 632 (1964); (b) T. H. Dunning and V. McKoy, J. Chem. Phys. 47, 1735 (1967); (c) A. D. McLachlan and M. A. Ball, Rev. Mod. Phys. 36, 844 (1964). See also Ref. (32) and Gy. Csanak, J. Phys. B 7, 1289 (1974) and references therein.

[48]E. U. Condon and G. H. Shortley, *The Theory of Atomic Spectra* (Cambridge University Press, New York, 1935), pp. 201–315 discusses importance of spin-orbit coupling for rare-gas spectra. See also G. Racah, Phys. Rev. 61, 537 (1942); R. H. Garstang and J. Van Blerkom, J. Opt. Soc. Am. 35, 1054 (1965).

[49]Spin-orbit coupling effects in the free-electron wave function were considered in a DWA calculation for electron-mercury scattering by D. H. Madison and W. N. Shelton, Phys. Rev. A 7, 514 (1973).

[50]In the RPA, the transition density matrix is calculated

directly, without the prior calculation of the wave functions involved.

[51]The term "configuration" is used here as defined by E. U. Condon and G. H. Shortley, Ref. 48.

[52]D. R. Hartree and W. Hartree, Proc. R. Soc. London Ser A 166, 450 (1938).

[53]R. S. Knox, Phys. Rev. 110, 375 (1958).

[54]J. R. Swanson and L. Armstrong, Jr., Phys. Rev. A 15, 661 (1977).

[55]D. Ton-That and L. Armstrong, Jr., Bull. Am. Phys. Soc. 24, 775 (1979) and private communication from Dr. D. Ton-That.

[56]The second equation of Ref. 53 is solved for the 4s orbital with $M=1$, using for all other orbitals the ground state HF value. [This defines the fixed-core HF (FCHF) approximation for the 4s orbital.]

[57]This assumption simplifies the analytical calculation to a great extent. In a future study, this restriction will be removed.

[58]R. D. Cowan and K. L. Andrew, J. Opt. Soc. Am. 55, 502 (1965).

[59]R. D. Cowan, J. Opt. Soc. Am. 58, 808 (1968); 58, 924 (1968).

[60]A. R. Edmonds, *Angular Momentum in Quantum Mechanics*, (Princeton University Press, Princeton, N. J., 1960), pp. 19-25.

[61]The definition and notation of Ref. 48 was adopted. See Ref. 48, pp. 37–45.

[62]F. J. da Paixão, N. Padial, and Gy. Csanak (unpublished).

[63]D. C. Cartwright, A. Chutjian, S. Trajmar, and W. Williams, Phys. Rev. A 16, 1013 (1977); D. C. Cartwright, A. Chutjian, and S. Trajmar, *ibid.* 16, 1041 (1977).

[64]D. C. Cartwright, J. Appl. Phys. 49, 3855 (1978).